Journal of Theoretical and Applied Mechanics, Sofia, 2011, vol. 41, No. 3, pp. 31–42

FLUID MECHANICS

COUPLED KELVIN-HELMHOLTZ AND TEARING MODE INSTABILITIES IN THE MAGNETOPAUSE LAYER*

S. Ivanovski
INAF – Osservatorio Astronomico di Capodimonte, Salita Moiariello 16, 80131 Naples, Italy

M. Kartalev, P. Dobreva, G. Vatkova
Institute of Mechanics, Bulgarian Academy of Sciences, Acad. G. Bontchev St., Bl. 4, 1113 Sofia, Bulgaria,
e-mails: m_kartalev@yahoo.com, polya2006@yahoo.com

T. Chernogorova
Sofia University, Faculty of Mathematics and Informatics, 5, James Bourchier Blvd, 1164, Sofia, Bulgaria,
e-mail: chernogorova@fmi.uni-sofia.bg

[Received 10 August 2011. Accepted 03 October 2011]

Abstract. We report results from numerical simulations of the coupled Kelvin-Helmholtz (KH) and tearing mode (TM) instability on the dayside magnetopause layer. We use our earlier proposed numerical scheme utilized in time-dependent two-dimensional approach for solving incompressible MHD equations with three dimensional velocity and magnetic field vectors and with magnetic and fluid viscosities included. Numerical tests with different sets of dimensionless input parameters are performed. The focus is on deriving conditions which lead to the development of the most intensive twin-vortex structures of the computed electric current systems. The computational domain in this context is taken to lie on the equatorial magnetopause region. The inferred instabilities could be candidates for causing mechanism of experimentally observed transient events such as the traveling convective vortices, detected in the ionosphere and on the ground.
Key words: magnetopause, instabilities, traveling convection vortices.

1. Introduction

The problem of modeling the dayside magnetopause instabilities by means of the fluid approach, as one of the successful methods for studying

*Corresponding author e-mail: polya2006@yahoo.com

such a task, has been intensively exploited during more than two decades (e.g. [11, 12], [17, 18], [1], [4], [5], [10]). The efforts of many researchers have been devoted to phenomena of the dayside transient events in the high-latitude ionosphere and magnetosphere, and especially of the so-called Traveling Convection Vortices (TCV), named recently also Magnetic Impulse Events (MIE) (e.g. [6], [7], [13], [8], [9], [2], [3]). Quite different and controversial opinions exist about the nature and the origin of these phenomena with possibly prevailing concept about their magnetopause, instability-related origin. The traveling convection vortices (TCVs) are dayside, transient type events observed at high latitudes in ground magnetometer records. They consist of a series of vortical ionospheric currents, traveling away from local noon tailward (westward in the morning sector). Usually it is assumed, that field-aligned currents at the center of each vortex couple perturbations from the magnetopause to the ionosphere, thus they are supposed to be possible ionospheric signatures as a result of the solar wind magnetosphere coupling processes.

A twin-vortex structures are likely to emerge under some appropriate conditions. Oppositely rotating cells of current vortices are created by a pair of upward and downward flowing field aligned currents. It was investigated in [14, 15] the twin structure of the vortex system by means of a fluid mechanics approach, instead of the more customary electromagnetic approach. These authors proved, that in the propagation around the polar cup boundary the traveling ionospheric vortices transport both momentum and magnetic flux in the direction of their phase velocity. Thus multiple disturbances could conceivably transport an important fraction of the polar cup magnetic flux from the dayside to the tail.

The aim of the present paper is an attempt to determine solar wind parameters (especially IMF direction in YZ plane), which are favorable in developing magnetopause instabilities, generating this interesting class of vortices with alternating directions.

2. Review of the applied model

The model, used to describe the flow dynamics of the magnetopause mixing layer in a fluid limit, is earlier proposed by [16]. The simulation domain (Fig. 1) consists of a rectangular region in (x, z)-plane, which is defined on locally introduced Cartesian grid, neglecting the realistic curvature, with coordinate x pointing direction along the velocity of the incident magnetosheath flow; z is in the direction downward to the Earth's center (from the magnetosheath to the magnetosphere) and y-direction is ensuring a right-handed coordinate system. The governing MHD equations are for incompressible, viscous, electrically-conductive fluid with the following restriction: the derivatives of all the parameters along y-direction are assumed to be zero. In dimensionless form this system reads:

$$
\begin{aligned}
\frac{\partial \rho}{\partial t} &= -u\frac{\partial \rho}{\partial x} - w\frac{\partial \rho}{\partial z},\\
\frac{\partial \Omega}{\partial t} &= -u\frac{\partial \Omega}{\partial x} - w\frac{\partial \Omega}{\partial z} + \frac{1}{R_e}\left(\frac{\partial^2 \Omega}{\partial x^2} + \frac{\partial^2 \Omega}{\partial z^2}\right) + \\
&\quad \frac{1}{M_A^2}\frac{1}{\rho}\left[B_x\frac{\partial J_y}{\partial x} + B_z\frac{\partial J_y}{\partial z} - \frac{J_y}{\rho}\left(B_x\frac{\partial \rho}{\partial x} + B_z\frac{\partial \rho}{\partial z}\right) + \frac{B_y}{\rho}\left(J_x\frac{\partial \rho}{\partial x} + J_z\frac{\partial \rho}{\partial z}\right)\right],\\
\frac{\partial v}{\partial t} &= -u\frac{\partial v}{\partial x} - w\frac{\partial v}{\partial z} + \frac{1}{R_e}\left(\frac{\partial^2 v}{\partial x^2} + \frac{\partial^2 v}{\partial z^2}\right) + \frac{1}{M_A^2}\frac{1}{\rho}\left(B_x\frac{\partial B_y}{\partial x} + B_z\frac{\partial B_y}{\partial z}\right),\\
\frac{\partial B_x}{\partial t} &= -u\frac{\partial B_x}{\partial x} - w\frac{\partial B_x}{\partial z} + \frac{1}{R_m}\left(\frac{\partial^2 B_x}{\partial x^2} + \frac{\partial^2 B_x}{\partial z^2}\right) + B_x\frac{\partial u}{\partial x} + B_z\frac{\partial u}{\partial z}, \qquad (1)\\
\frac{\partial B_y}{\partial t} &= -u\frac{\partial B_y}{\partial x} - w\frac{\partial B_y}{\partial z} + \frac{1}{R_m}\left(\frac{\partial^2 B_y}{\partial x^2} + \frac{\partial^2 B_y}{\partial z^2}\right) + B_x\frac{\partial v}{\partial x} + B_z\frac{\partial v}{\partial z},\\
\frac{\partial B_z}{\partial t} &= -u\frac{\partial B_z}{\partial x} - w\frac{\partial B_z}{\partial z} + \frac{1}{R_m}\left(\frac{\partial^2 B_z}{\partial x^2} + \frac{\partial^2 B_z}{\partial z^2}\right) + B_x\frac{\partial w}{\partial x} + B_z\frac{\partial w}{\partial z},\\
\Omega &= \nabla^2\phi; \quad \mathbf{V} = -\nabla\times(\phi\mathbf{e}_x),\\
\mathbf{j} &= \nabla\times\mathbf{B},
\end{aligned}
$$

where ϕ is a streamline function, u, v, w are components of the velocity vector $\mathbf{V}$; B_x, B_y, B_Z are components of the magnetic field vector $\mathbf{B}$; $\mathbf{\Omega}$ and $\mathbf{j}$ are fluid vorticity and electric current density; $R_e = \tilde{V}\tilde{L}/\nu$ and $R_m = \tilde{V}\tilde{L}/\nu_m$ are Reynolds and magnetic Reynolds numbers, M_A is Alfven Mach number and ρ is density.

Parameters' scales are chosen as follows: $\tilde{\rho}$, $\tilde{V}$ – those of the unperturbed solar wind; $\tilde{L} = L_x$ – length scale of the imposed perturbation; $\tilde{t} = \tilde{L}/\tilde{V}$; $\tilde{B}$ – inner (magnetospheric) magnetic field on the magnetopause.

Periodic boundary conditions are adopted for all input quantities in the horizontal x-direction. In z-direction, "soft" boundary conditions for v, w, B_z and ρ are chosen:

$$\frac{\partial v}{\partial z} = \frac{\partial w}{\partial z} = \frac{\partial B_z}{\partial z} = \frac{\partial \rho}{\partial z} = 0,$$

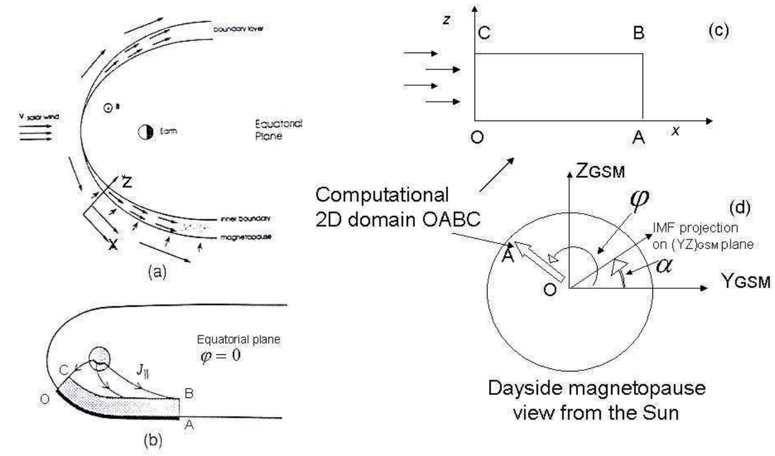

Fig. 1. Qualitative sketch of the position of the applied 2D computational region. (The left panel is after [18])

and fixed conditions for the rest of the parameters u, Ω, B_x and B_y:

$$u\Big|_{z=0} = V^{sh}\ ,\ \ u\,|_{z=L_z} = 0\ ,\ \ \Omega\,|_{z=0} = \Omega\,|_{z=L_z} = 0,$$

$$B_x\,|_{z=0} \equiv B_x^{sh},\ \ B_x\,|_{z=L_z} \equiv B_x^{mg},\ \ B_y\,|_{z=0} \equiv B_y^{sh},\ \ B_y\,|_{z=L_z} \equiv B_y^{mg}.$$

The conditions for ϕ result from those for Ω and $\mathbf{V}$.

The initial parameters' distributions are supposed to be undependable on x, which implies the following initial z-profiles:

$$\begin{aligned}
u^o(z) &= \frac{1}{2}V_0\left(1-\tanh\frac{z-0.5L_z}{\nu_u}\right),\\
v^o(z) &\equiv 0,\quad w^o(z)\equiv 0,\quad B_z^o(z)\equiv 0,\\
B_x^o(z) &= \frac{B_x^{mg}-B_x^{sh}}{2}\tanh\left(\frac{z-0.5L_z}{\nu_B}\right)+\frac{B_x^{mg}-B_x^{sh}}{2},\\
B_y^o(z) &= \frac{B_y^{mg}-B_y^{sh}}{2}\tanh\left(\frac{z-0.5L_z}{\nu_B}\right)+\frac{B_y^{mg}-B_y^{sh}}{2},\\
\rho^o(z) &= \frac{1}{2}(\rho^{sh}+\rho^{mg})-\frac{1}{2}(\rho^{sh}-\rho^{mg})\tanh\left(\frac{z-0.5L_z}{\nu_\rho}\right),
\end{aligned} \qquad (2)$$

where ρ^{sh}, $\mathbf{B}^{sh}$ and ρ^{mg}, $\mathbf{B}^{mg}$ are prescribed densities and magnetic fields at the magnetosheath and magnetospheric sides respectively, L_z represents the magnetopause border in the model and ν_ρ,ν_u, ν_B specify the "thickness" of the initial distributions of the density, velocity and the magnetic field respectively.

The adopted profiles provide self-consistent initial distributions for Ω and ϕ:

$$\begin{aligned} \phi^o(z) &= \frac{1}{2}V_0\left(z-\nu_u \ln\left(\cosh\frac{z-0.5L_z}{\nu_u}\right)+\nu_u\ln(\cosh(-0.5L_z/\nu_u))\right), \\ \Omega^o(z) &= -\frac{1}{2}\frac{V_0}{\nu_u}\frac{1}{cosh^2\left(\frac{z-0.5L_z}{\nu_u}\right)}. \end{aligned} \tag{3}$$

The initial disturbance of the parameter $\mathbf{X}$ is given by:

$$\mathbf{X}_\delta(x,z) = \mathbf{X}^o(z) + \omega^* \sin\left(\frac{2\pi x}{L_x}\right)\exp\left(-\frac{(z-0.5L_z)^2}{\nu_u^2}\right), \tag{4}$$

with an appropriate amplitude ω^*.

In the numerical simulations in Section 3 the initial disturbance is posed on the vorticity. The "thickness" parameters ν_u and ν_B are prescribed to be 0.04 and 0.02, respectively. The details of the finite difference numerical scheme will be presented elsewhere. The uniform grid (65×65) is used in all simulations.

3. Some numerical results

The used approach is flexible enough to imitate any position on the dayside magnetopause by posing appropriate boundary conditions (Fig. 1), provided that the magnetosheath solution is available. Some approximate estimates are possible even without using the later solution because of the "simple" behavior of the velocity and the density around the magnetopause and the approximate maintaining near the magnetopause of the IMF projection on YZ plane as well. The solution provides the time evolution (stability/instability) of all the parameters, perturbed with the initial disturbance, as well as the "traveling" velocity of the created configurations (usually vortical).

In this study we are interested specifically on the j_y component (in the computational coordinate system), which coincides in our model with the Z^{GSM} component of the electric current vector $\mathbf{j}$. Choosing $\varphi = 0$ (Fig. 1), the computational Y- direction coincides with the Earth's magnetic field line

(Z^{GSM}-direction), and thus, the computed current components are supposed to be directly mapped onto the polar ionosphere. The goal of this paper is not a systematic study over all the spectrum of all possible solar wind conditions, but we would rather present a few particular, but informative tendencies, dealing here only with dimensionless parameters.

The dimensionless boundary conditions from the magnetosphere side (CB side of the rectangular OABC in Fig. 1) are taken everywhere to be identical: $B_y^{mg} = 1.0$, $B_x^{mg} = B_x^{mg} = 0$, $\mathbf{V}^{mg} = 0$, $\rho^{mg} = 0.1$. From the magnetosheath side (OA side of the rectangular OABC in Fig. 1), $\rho^{sh} = 1.0$ everywhere and some tendencies with varying velocity and magnetic field boundary conditions are discovered. The only well sought effect in the present study is the development of j_y (j_z in GSM) vortically organized filaments with alternating vortex signs and with comparable intensities of the neighboring "up" and "down" vortical current systems. This effect could be concisely named Twin Vortices (TV) effect. Note that so described computational problem statement corresponds to the afternoon sector and eastward (tail-ward) movement of the mapped current filaments configurations. The analogical case with $\varphi = \pi$, providing generally mirror-symmetric results, is not presented here.

The dependence of the developed coupled KH and TM instabilities on the orientation of the IMF projection $\mathbf{B}_{yz}^{GSM}$ in the YZ^{GSM} plane is presented in Fig. 2, where $V^{sh} = 1.0$ (see the figure caption for more details). It shows, that the created vortices are mostly with the same sign (only "up" or only "down"). If an opposite vortex appears, it is with a negligible intensity, i.e. the maximum is about $j_z^{GSM} \sim 3.7$ and the minimum value is about $j_z^{GSM} \sim 0.05$ in the plot **d** (north-west $\mathbf{B}_{yz}^{GSM}$ direction). The most considerable candidates for a created TV structure are the cases – f (south-west $\mathbf{B}_{yz}^{GSM}$ direction), where the maximum is $j_z^{GSM} \sim 3.9$ and the minimum is $j_z^{GSM} \sim 1.2$, and also the plot h (south-east $\mathbf{B}_{yz}^{GSM}$ direction).

Quite different picture appears in Fig. 3, where all the conditions are the same as in Fig. 2, but with the only exception as follows: we have a smaller value for the magnetosheath side dimensionless velocity ($V^{sh} = 0.3$), which qualitatively means, that the computational domain is much closer to the subsolar magnetopause point (stagnation point). From the "ionospheric point of view" the mapped current configurations are supposed to be closer to the local noon. Well expressed twin vortices structures appear when nonzero Y-component of $\mathbf{B}_{yz}^{GSM}$ exists alone (plots **a**, **e**), or accompanied with its negative Z-component (plots **f**, **h**). The stronger TV-effect appears again in the south-east sector (plot **h**), where the maximum value $j_z^{GSM} \sim 6.58$ and the minimum $j_z^{GSM} \sim -5.97$.

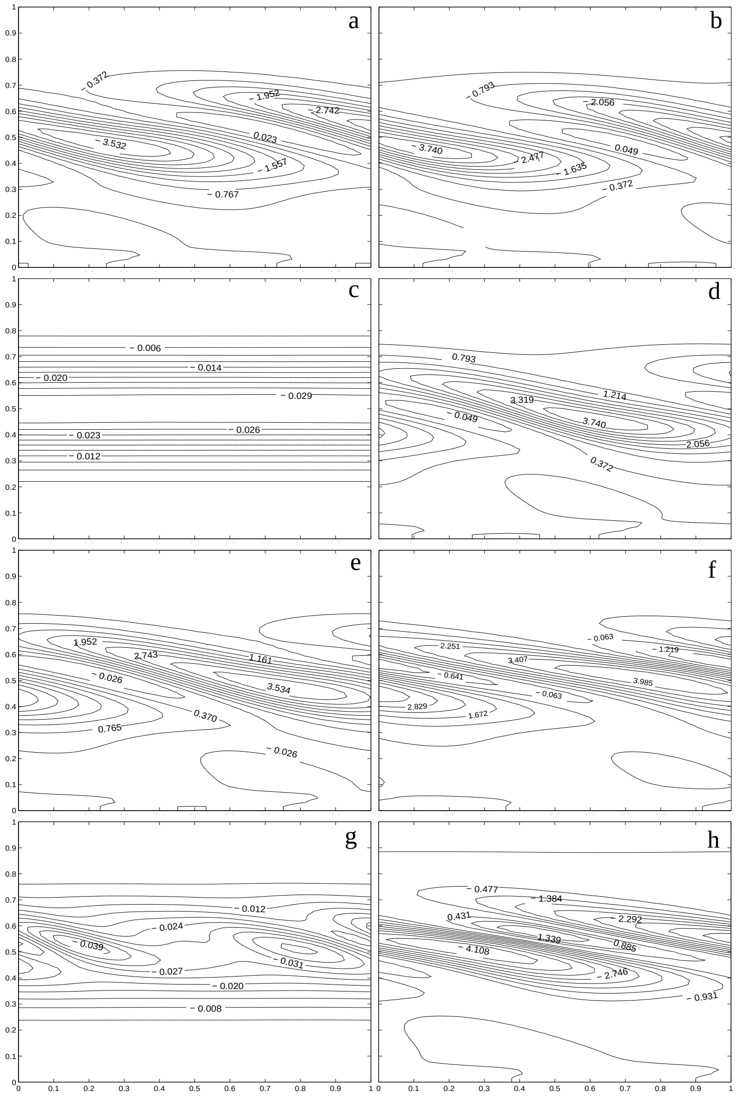

Fig. 2. Dependence of the developed coupled Kelvin Helmholtz and tearing mode instabilities on the orientation of the IMF projection $\mathbf{B}_{yz}^{GSM}$ in the YZ^{GSM} plane. Each plot presents isoline contours of the j_z^{GSM} values. The computational domain corresponds to $\varphi = 0$ in Fig. 1 (see the text). The $\mathbf{B}_{yz}^{GSM}$ direction, given by the angle α (Fig. 1) varies as follows: $\alpha = n\pi/4$, $n = (0, 1, 2, 3, 4, 5, 6, 7)$ in the panels (a, b, c, d, e, f, g, h), respectively. The specific dimensionless boundary conditions (see the text) are: $V^{sh} = 1.0$; the absolute value of the posed as a boundary condition on the magnetosheath side magnetic field is everywhere $|\mathbf{B}_{yz}^{GSM}| = 8.5$

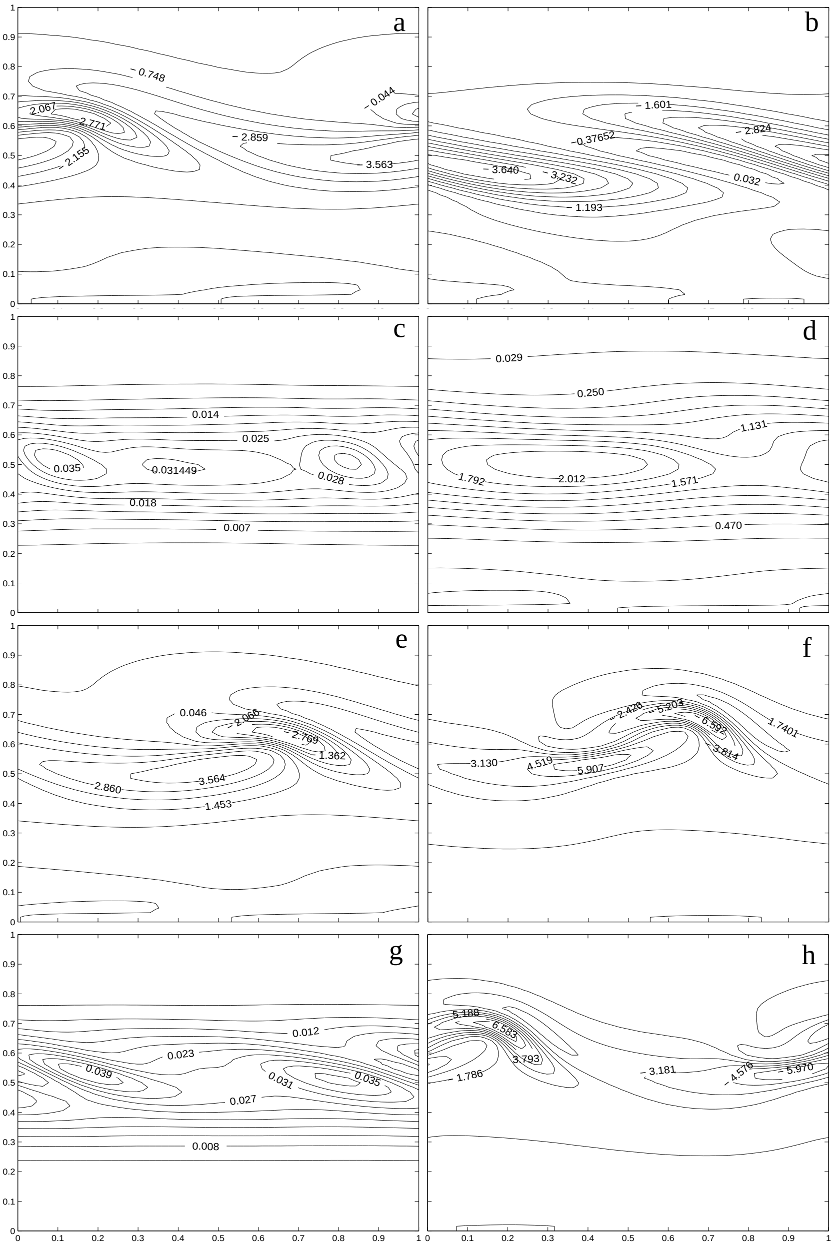

Fig. 3. The same as in Fig. 2, but with dimensionless velocity boundary condition on the magnetosheath side: $V^{sh} = 0.3$

Table 1. Some tendencies in the dependence of the twin vortex effect on the IMF direction and the distance from the subsolar magnetopause point. The TV effect is expressed via the values of the strongest upward and downward currents ($\max j_z^{GSM}$ and $\min j_z^{GSM}$, respectively). The values are obtained running the model for the $\mathbf{B}_{yz}^{GSM}$ south-east quadrant (angle $\alpha = -\pi/4$ in Fig.) applying two different values for V^{sh} – the dimensionless velocity boundary condition on the magnetopause side and three different values of $|\mathbf{B}|^{sh}$

V^{sh}	0.3	0.3	0.3	1.0	1.0	1.0
$\|\mathbf{B}\|^{sh}$	0.35	0.7	1.0	0.35	0.7	1.0
$\min j_z^{GSM}$	-5.59	-6.96	-4.69	-2.21	-3.74	-3.86
$\max j_z^{GSM}$	5.25	10.88	4.08	0.25	1.80	-0.05

We present in Table 1 a comparison between $\max j_z^{GSM}$ and $\min j_z^{GSM}$ values obtained for the south-east quadrant of the $\mathbf{B}_{yz}^{GSM}$ direction (angle $\alpha = -\pi/4$ in Fig. 1. The table gives a very approximate idea about some tendencies in the dependence of the twin vortex effect on the IMF direction and on the distance from the subsolar magnetopause point, i.e. the effect is stronger for smaller value of V^{sh} (nearer the noon). The dependence on $|\mathbf{B}|^{sh}$ is not a simple one. Thus the maximum effect is reached for some intermediate value among the investigated values.

Some examples of the instability patterns developed by other parame-

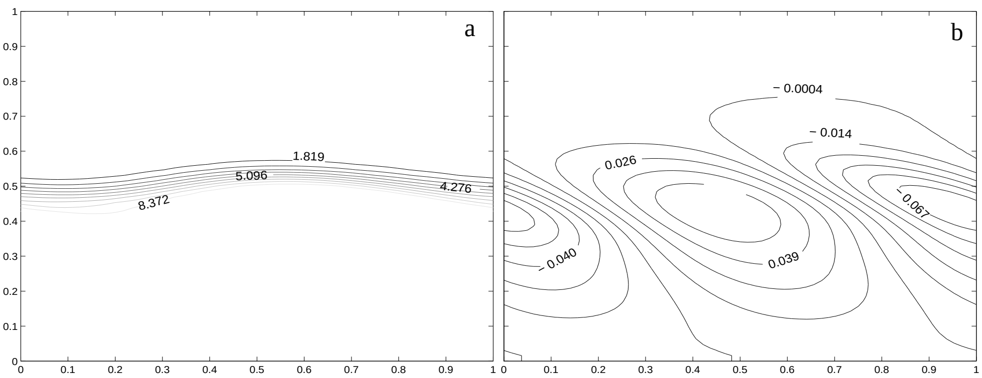

Fig. 4. Illustration of the developed instability in some other parameters in the case of a weak twin vortices effect (case (b) in Fig. 3). a)Contour plot of the isolines of the dimensionless density ρ; b) Dimensionless ("computational") B_z component, directed locally downward to the Earth's center

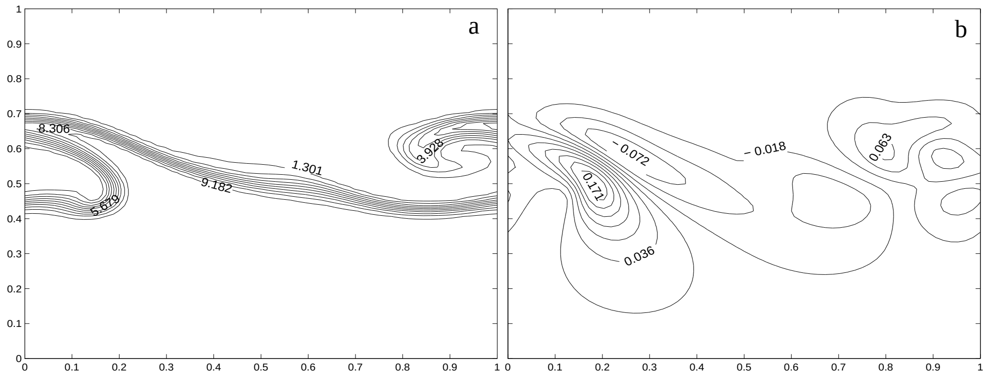

Fig. 5. The same as in Fig. 4, but in the case of a strong twin vortices effect – plot f in Fig. 3

ters (Figs 4 and 5), demonstrate the flexibility of our approach, which is balancing intrinsically the Kelvin-Helmholtz and tearing mode instability effects depending on the posed conditions.

4. Summary

A flexible numerical incompressible MHD approach is presented and implemented for studying a coupled Kelvin-Helmholtz (KH) and tearing mode (TM) instability. A full 3D MHD system for incompressible and conducting fluid is reduced only by neglecting the partial derivatives in one direction. The instabilities within the dayside magnetopause mixing layer are modeled numerically by introducing an appropriate initial parameters' distribution and sharp initial disturbance. In this study, we were focused only on the created vortical configurations in the distribution of the electric current component, aligned alone the Earth's magnetic field lines and thus, mapped to the polar ionosphere. It seems that "twin vortices" effect, characterized by "up/down" alternating vortices is strongest for south-east directed IMF and nearer to the subsolar point, corresponding to the noon in the ionosphere.

Acknowledgments. This work is supported by the European Social Fund and Bulgarian Ministry of Education, Youth and Science under Operative Program "Human Resources Development", Grant BG051PO001-3.3.04/40. This research was also partially supported by the Bulgarian National Council Scientific Research under project NZ-1315/03. MK was supported by the Air Force Office of Scientific Research, Air Force Material Command, USAF, under grant FA8655-05-1-3024.

REFERENCES

[1] Chen, Q., A. Otto, L. C. Lee. Tearing Instability, Kelvin-Helmholtz Instability, and Magnetic Reconnection. *J. Geophys. Res.*, **102** (1997), No. **A1**, 151–161.

[2] Clauer, C. R., V. G. Petrov. A Statistical Investigarion of Traveling Convection Vortices Observed by the West Coast Greenland Magnetometer Chain. *J. Geophys. Res.*, **107** (2002), No. **A7**, doi:10.1029/2001JA000228.

[3] Kataoka, R., H. Fukunishi, L. J. Lanzerotti, T. J. Rosenberg, A. T. Watherwax, M. J. Engebretson, J. Watermann. Traveling Convection Vortices Induced by Solar Wind Tangential Discontinuities. *J. Geophys. Res.*, **107** (2002), No. **A12**, 1455, doi:10.1029/2002JA009459.

[4] Keller, K. A., R. L. Lysak. A Two-dimensional Simulation of the Kelvin-Helmholtz Instability with Magnetic Shear. *J. Geophys. Res.*, **104** (1999), No. **A11**, 25097–25103.

[5] La Belle-Hamer, A. L., A. Otto, L. C. Lee. Magnetic Reconnection in the Presence of Sheared Flow and Density Asymmetry: Applications to the Earths Magnetopause. *J. Geophys. Res.*, **100** (1995), No. **A7**, 11875–11889.

[6] McHenry, M. A., C. R. Clauer, E. Friis-Christensen, P. T. Newwell, J. D. Kelly. Ground Observations of Magnetospheric Boundary Layer Phenomena. *J. Geophys. Res.*, **95** (1990a), No. **A9**, 14995–15005.

[7] McHenry, M. A., C. R. Clauer, E. Friis-Christensen. Relationship of Solar Wind Parameters to Continuous, Dayside, High Latitude Traveing Ionospheric Convection Vortices. *J. Geophys. Res.*, **95** (1990b), No. **A9**, 15007–15022.

[8] Moretto, T., E. Friis-Christensen, H. Luhr, E. Zesta. Global Perspective of Ionospheric Travelling Convection Vortices: Case Studies of Two Geospace Environmental Modeling Events. *J. Geopgys. Res.*, **102** (1997), No. **A6**, 11597–11610.

[9] Moretto, T., M. Hesse, A. Yahnin, A. Ieda, D. Murr, F. Watermann. Magnetospheric Signature of an Ionospheric Traveling Convection Vortex Event. *J. Jeophys. Res.*, **107** (2002), No. **A6**, doi:10.1029/2001JA000049.

[10] Otto, A., D. H. Fairfield. Kelvin-Helmholtz Instability at the Magnetotail Boundary: MHD Simulation and Comparison with Geotail Observations. *J. Geophys. Res.*, **105** (2000), No. **A9**, 21175–21190.

[11] Pu, Z. Y., M. Yei, Z. X. Liu. Generation of Vortex-induced Tearing Mode Instability at the Magnetopause. *J. Geophys. Res.*, **95** (1990a), No. **A7**, 10559–10566.

[12] Pu, Z. Y., P. T. Hou, Z. X. Liu. Vortex-induced Tearing Mode Instability as a Source of Flux Transfer Events. *J. Geophys. Res.*, **95** (1990b), No. **A11**, 18861–18869.

[13] Sitar, R. J., J. B. Baker, C. R. Clauer, A. J. Ridley, J. A. Cumnok, V. O. Papitashvili, J. Spann, M. J. Brittnacher, G. K. Parks. Multi-instrument Analysis of the Ionosphere Signatures of a Hot Flow Anomaly Occurring on July 24, 1996. *J. Geophys. Res.*, **103** (1998), No. **A10**, 23357–23372.

[14] Southwood, D., M. Kivelson. An Approximate Description of Field-aligned Currents in a Planetary Magnetic Field. *J. Geophys. Res.*, **96** (1991), No. **A1**, 67–75.

[15] Southwood, D., M. Kivelson. Vortex Motion of the Ionosphere and Nonlinear Transport. *J. Geophys. Res.*, **98** (1993), No. **A7**, 11459–11466.

[16] Vatkova, G., M. Kartalev. Numerical Simulation of the Nonlinear Instabilities in the Magnetopause Layer. *Journal of Theoretical and Applied Mecahnics*, Vol. **30** (2000), No. **2**, 50–62.

[17] Wei, C. Q., L. C. Lee, La A. L. Belle-Hamer. A Aimulation Study of the Vortex Structure in the Low-latitude Boundary Layer. *J. Geophys. Res.*, **95** (1990), No. **A12**, 20793–20807.

[18] Wei, C. Q., L. C. Lee. Coupling of Magnetopause-boundary Layer to the Polar Ionosphere. *J. Geophys. Res.*, **98** (1993), No. **A4**, 5707–5725.